AFRL-AFOSR-UK-TR-2020-0021

Understand the Chiral Selectivity of Single-Walled Carbon Nanotube growth by in situ optical imaging of individual and identified carbon nanotubes

Vincent Jourdain
CTRE NAT DE LA RECHERCHE SCIENTIFIQUE
1919, ROUTE DE MENDE
MONTPELLIER, 34000
FR

06/23/2020
Final Report

Air Force Research Laboratory
Air Force Office of Scientific Research
European Office of Aerospace Research and Development
Unit 4515 Box 14, APO AE 09421

REPORT DOCUMENTATION PAGE

Form Approved
OMB No. 0704-0188

1. REPORT DATE *(DD-MM-YYYY)*	2. REPORT TYPE	3. DATES COVERED *(From - To)*
23-06-2020	Final	01 Dec 2016 to 28 Feb 2019

4. TITLE AND SUBTITLE
Understand the Chiral Selectivity of Single-Walled Carbon Nanotube growth by in situ optical imaging of individual and identified carbon nanotubes

5a. CONTRACT NUMBER

5b. GRANT NUMBER
FA9550-17-1-0027

5c. PROGRAM ELEMENT NUMBER
61102F

6. AUTHOR(S)
Vincent Jourdain

5d. PROJECT NUMBER

5e. TASK NUMBER

5f. WORK UNIT NUMBER

7. PERFORMING ORGANIZATION NAME(S) AND ADDRESS(ES)
CTRE NAT DE LA RECHERCHE SCIENTIFIQUE
1919, ROUTE DE MENDE
MONTPELLIER, 34000 FR

8. PERFORMING ORGANIZATION REPORT NUMBER

9. SPONSORING/MONITORING AGENCY NAME(S) AND ADDRESS(ES)
EOARD
Unit 4515
APO AE 09421-4515

10. SPONSOR/MONITOR'S ACRONYM(S)
AFRL/AFOSR IOE

11. SPONSOR/MONITOR'S REPORT NUMBER(S)
AFRL-AFOSR-UK-TR-2020-0021

12. DISTRIBUTION/AVAILABILITY STATEMENT
A DISTRIBUTION UNLIMITED: PB Public Release

13. SUPPLEMENTARY NOTES

14. ABSTRACT
Single-walled carbon nanotubes (SWCNTs) have received tremendous attention since their discovery due to the combination of exceptional properties. However, the development of SWCNT-based technologies is hindered by the mixture of SWCNTs with different structures and properties in as-grow samples. To address this issue, our objective was to measure the growth kinetics of individual SWCNTs using a new imaging method named homodyne polarized optical microscopy (HPOM), and to correlate them with their structure independently measured by optical spectroscopies. Our first study was devoted at improving the understanding of HPOM spectra: we developed a model which allows to separate the intrinsic nanotube features from the contributions of the substrate and the optics. Our second study was devoted at demonstrating that individual SWCNTs can be imaged using HPOM under real growth conditions: it evidenced that individual SWCNTs grow at a constant growth rate until sudden termination. The lifetime also appears inversely related to the growth rate, which supports that the limiting step of nanotube growth is also responsible for the sudden termination. Finally, our third study was devoted to relating the growth kinetics of individual SWCNTs with their structure. It revealed that the growth rate is minimal for chiral angles of 19 and maximum for zigzag and armchair SWCNTs. Based on the correlation with defect density and observations of nanotube etching, this is rationalized by a competition at the nanotube edge between carbon integration and chiral-selective etching.

15. SUBJECT TERMS
carbon nanotube, SWCNT, manufacturing

16. SECURITY CLASSIFICATION OF:			17. LIMITATION OF ABSTRACT	18. NUMBER OF PAGES	19a. NAME OF RESPONSIBLE PERSON
a. REPORT	b. ABSTRACT	c. THIS PAGE			FOLEY, JASON
Unclassified	Unclassified	Unclassified	SAR		19b. TELEPHONE NUMBER *(Include area code)* 011-44-1895-616036

Standard Form 298 (Rev. 8/98)
Prescribed by ANSI Std. Z39.18

FINAL TECHNICAL REPORT

Understand the Chiral Selectivity of Single-Walled Carbon Nanotube growth by in situ optical imaging of individual and identified carbon nanotubes

Grant FA9550-17-1-0027

Title: Understand the selectivity of SWCNT growth by in situ optical imaging and spectroscopy

Principal investigator: Vincent Jourdain, Associate Professor

Affiliation: Laboratoire Charles Coulomb (CNRS-Université de Montpellier)

Contact details: Laboratoire Charles Coulomb, Place Bataillon, 34095 Montpellier Cedex 5, France. E-mail: vincent.jourdain@umontpellier.fr. Tel.: +33 (0)4 67 14 47 78

Project duration (in months): 27 (from 1 December 2016 to 28 February 2019)

Abstract (< 250 words):

Single-walled carbon nanotubes (SWCNTs) have received tremendous attention since their discovery due to the combination of exceptional properties. However, the development of SWCNT-based technologies is hindered by the mixture of SWCNTs with different structures and properties in as-grow samples. To address this issue, our objective was to measure the growth kinetics of individual SWCNTs using a new imaging method named homodyne polarized optical microscopy (HPOM), and to correlate them with their structure independently measured by optical spectroscopies. Our first study was devoted at improving the understanding of HPOM spectra: we developed a model which allows to separate the intrinsic nanotube features from the contributions of the substrate and the optics. Our second study was devoted at demonstrating that individual SWCNTs can be imaged using HPOM under real growth conditions: it evidenced that individual SWCNTs grow at a constant growth rate until sudden termination. The lifetime also appears inversely related to the growth rate, which supports that the limiting step of nanotube growth is also responsible for the sudden termination. Finally, our third study was devoted to relating the growth kinetics of individual SWCNTs with their structure. It revealed that the growth rate is minimal for chiral angles of 19° and maximum for zigzag and armchair SWCNTs. Based on the correlation with defect density and observations of nanotube etching, this is rationalized by a competition at the nanotube edge between carbon integration and chiral-selective etching.

Keywords: carbon nanotubes, growth, CVD, in situ, optical imaging, chiral selectivity, catalytic etching

1. Context and objectives of the project

Single-walled carbon nanotubes (SWCNTs) have received tremendous attention since their discovery due to the combination of exceptional electrical, thermal, optical and mechanical properties. SWCNTs can be either metallic or semiconducting depending on their structure (also called chirality): metallic SWCNTs display electrical and thermal conductivities an order of magnitude higher than copper while semiconducting SWCNTs display electrical and optical properties extremely dependent on their chemical environment. On top of that, SWCNTs are very light, extremely strong and chemically resistant. The mass-production of SWCNTs has now been made possible by Catalytic Chemical Vapor Deposition (CCVD) using metal nanoparticles which catalyze the decomposition of a gaseous carbon source. However, the development of SWCNT-based technologies is still hindered by the fact that as-grown samples are mixtures of SWCNTs of different structures / chiralities and, therefore, of different physical properties.

Very early, SWCNTs have been envisioned for replacing Si but have been hampered by three major hurdles: the nanotube positioning, the contact resistance with the electrodes and the mixture of different chiralities. Key breakthroughs within the last years have radically changed this picture. First, lattice-oriented growth (*1*) on quartz and sapphire allows growing dense arrays (> 100 SWCNT / µm) of horizontally-aligned SWCNTs (HA-SWCNTs) (*2*). Using such HA-SWCNTs, Stanford researchers reported a SWCNT-based 3D-integrated processor incorporating more than 2 million SWCNT field-effect transistors (FETs) on a single chip (*3*). Second, IBM showed that the contact resistance can be suppressed by forming a carbide interface and therefore no more limits the downscaling of SWCNT devices (*4*). A striking example was reported by Peking University with a SWCNT-FET with 5-nm gate length and 25-nm contact length performing faster and at lower power than Si FETs of the same size (*5*). Third, new sorting methods allow preparing suspensions highly enriched in SC-SWCNTs. Using such suspensions, IBM reported high-performance ring oscillators (the standard benchmark for performance and technology maturity) with a switching frequency of 2.82 GHz (*6*). Following these engineering breakthroughs, SWCNTs now appear for many as one of the most mature solutions for building a novel generation of transistors both highly performant and energy-efficient. This is notably illustrated by IBM's announcement of their aim to have SWCNT-FETs ready for commercialization in the 2020s (*7*), and by the exponential increase in SWCNT research and manufacturing in China (*8*).

Currently, the main bottleneck for the development of SWCNT-based electronics is the lack of a base material with appropriate specifications. IBM researchers calculated that reaching the requirements of the international technology roadmap for semiconductors (ITRS) for the 2020s requires highly-aligned SWCNT arrays with density of ~100 SWCNT/µm and semiconductor purity higher than 99.9999% on a wafer scale (*9*). Shulaker *et al*. showed that this purity requirement can be partially alleviated by using architectures less vulnerable to metallic SWCNT impurities (*10*). Sorting methods in liquid phase already allowed the preparation of SWCNT arrays of 500 SWCNT/µm from SC-enriched solutions but these methods have a too low throughput for industrial needs and the device performances suffer from the insufficient SWCNT alignment and the short nanotube length (*11*). HA-SWCNT arrays directly grown with appropriate electronic properties (*e.g.* with a high purity in SC-SWCNTs with controlled bandgap) would represent a major breakthrough and a key industrial advantage compared with the low-yield and costly post-growth sorting methods. However, the best selectivity values reported so far for HA-SWCNTs are 91-97% of SC-SWCNTs (*12–14*). The central issue is that there is no clear understanding of the mechanisms governing the selectivity of SWCNT growth. Higher thermodynamic stability (*e.g.* chirality-dependent nucleation probability) (*15*, *16*), or preferential growth kinetics (*e.g.* chirality-dependent growth

rate or lifetime) (*16*, *17*) are generally invoked but the experimental verification of these hypotheses and of their predictions is essentially missing.

To address this issue, our project aimed at directly imaging the growth of individual SWCNTs in real CVD conditions in order to determine the kinetics of nucleation, growth and termination of each SWCNT chirality. To do so, we developed a new optical microscopy setup based on polarization extinction (*18*) which has the still world-unique ability to image individual SWCNTs under real conditions of growth (*i.e.* at atmospheric pressure on a substrate). These kinetic measurements were coupled with an identification of the structure of each SWCNT in order to determine the mechanisms underlying the selectivity for a specific type of tubes and given synthesis conditions.

2. Results

a. Modeling the optical response of individual SWCNTs on substrate during polarized microscopy experiments

Our first work (*18*) was devoted at improving the understanding of the processes governing the contrast of homodyne polarized optical microscopy (HPOM), the technique we aimed at using for imaging individual SWCNTs during their growth on substrate and measuring their optical spectrum.

Absorption is here the signal of choice because it displays by far the highest cross section of SWCNT optical features. However, it has long been impossible to measure the optical features of individual SWCNTs on a substrate because these are usually covered by the intense scattering and reflection by the substrate. Recently, novel optical methods have been developed to directly measure the optical features of individual nanotubes directly on substrates (*19–21*). Among them, homodyne polarized optical spectroscopy (*22–24*) is of particular interest since it imposes no additional constraint (e.g., deposited layer, liquid environment) on the sample. The method relies on the strong polarization effect of SWCNTs along their main axis. By setting the SWCNT between two crossed polarizers, at an angle of 45◦ with the main axes of the polarizers (Figure 1), the intense substrate signal which keeps the incident polarization can be reduced by several orders of magnitude, thus making the weak nanotube signal observable. However, the theoretical treatment is complicated by several factors which were not fully included in previous models. First, these models considered non-coherent depolarization by the optical system and neglects the possibility of coherent depolarization, which is needed to account for interferential features. Second, the complex-number nature of the reflection factor was not developed, which is especially important in the case of Si substrates with a thermal oxide layer (SiO_2) acting as an antireflection coating.

Our experimental study revealed that the polarized optical spectra of individual carbon nanotubes are actually more complex than described by previous models. The experimental spectra notably display different background shapes depending on the type of substrate and periodic fluctuations when working at very high extinction ratio (Figures 2a,b).

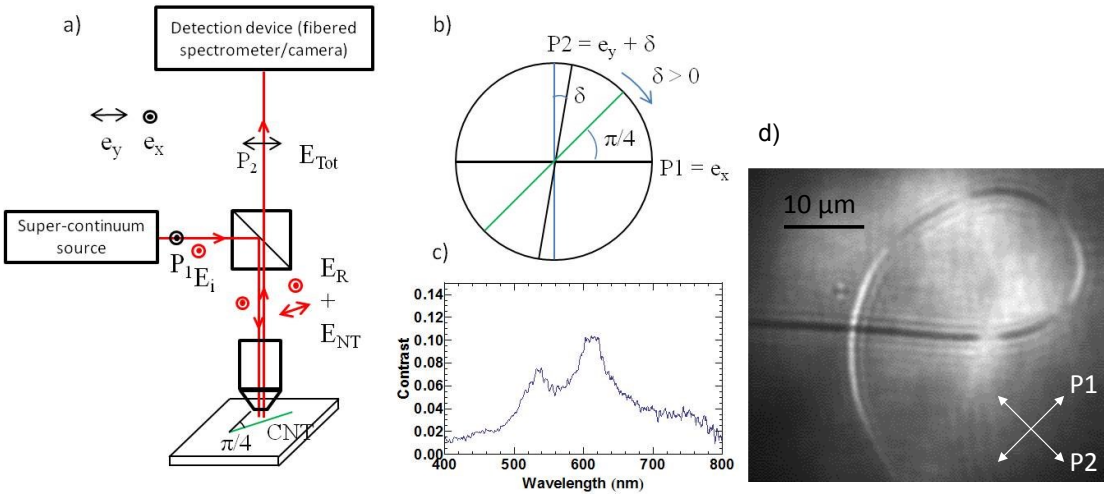

Figure 1. Polarization-based optical spectroscopy of individual carbon nanotubes on substrate. (a) Simplified schema of the experimental setup. (b) Cross polarizers configuration. Analyzer P_2 is set at an angle $\pi/2 - \delta$ with respect to the polarizer P_1 and the carbon nanotube (green line) is set at around $\pi/4$ with respect to the polarizers. (c) Typical experimental spectrum of a carbon nanotube on substrate measured with $\delta = 0.02$ rad. d) Optical image of a nanotube (loop) using the same setup.

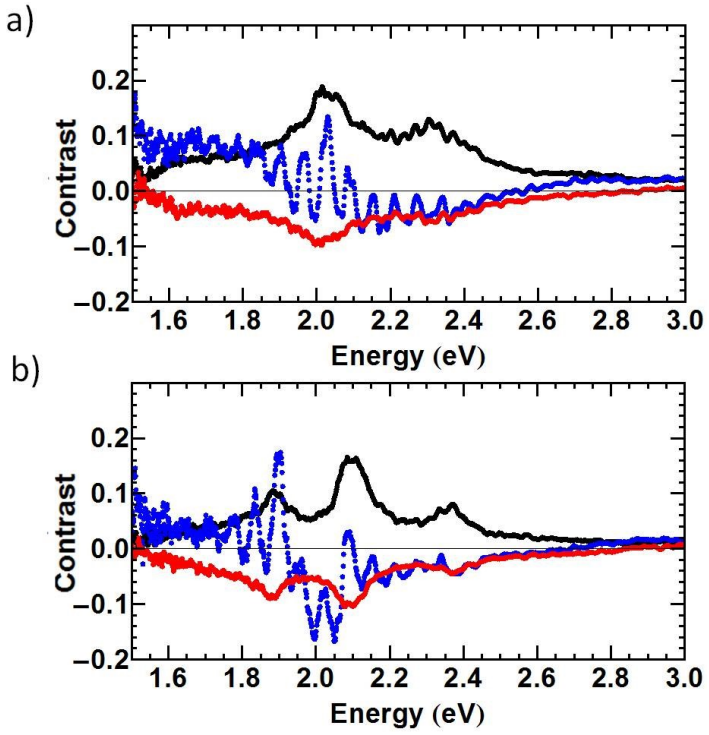

Figure 2. Experimental spectra of carbon nanotubes for three different angles δ: 10^{-2} (black), -5×10^{-3} (blue), and -5×10^{-2} (red) rad. (a) Case A. (b) Case B. In both cases, the substrate is 100 nm SiO_2/Si.

To account for these observations, we developed a model including both coherent and non-coherent depolarization by the optics, and the antireflection effect of the substrate. Importantly, we showed that the optical response of the substrate cannot be simply removed from the experimental spectra due to its coupling with the complex nanotube susceptibility and the coherent depolarization by the optics. We developed an experimental protocol to measure the depolarization parameters and showed that coherent depolarization is needed to correctly

fit all experimental spectra: it allows to reproduce the wavelength dependence of both the extinction ratio and the angle of maximum extinction, which would not be possible considering only non-coherent depolarization. Knowing the depolarization factors, our model allows to separate the intrinsic nanotube features from the contribution of the substrate and of the imperfect optics in the experimental spectra. Even though experimental details may be improved, the developed model allows to extract both the real and imaginary parts of the nanotube susceptibility even on substrates with an antireflection layer such as standard SiO_2/Si (Figure 3a,b). Finally, the method allows one to reconstruct the Rayleigh spectra of each SWCNT without the interference of optics depolarization and substrate effects (Figure 3c,d): these refined optical spectra can then be used to assist and consolidate the structural assignment of individual SWCNTs by combining with other techniques (*e.g.* Raman spectroscopy).

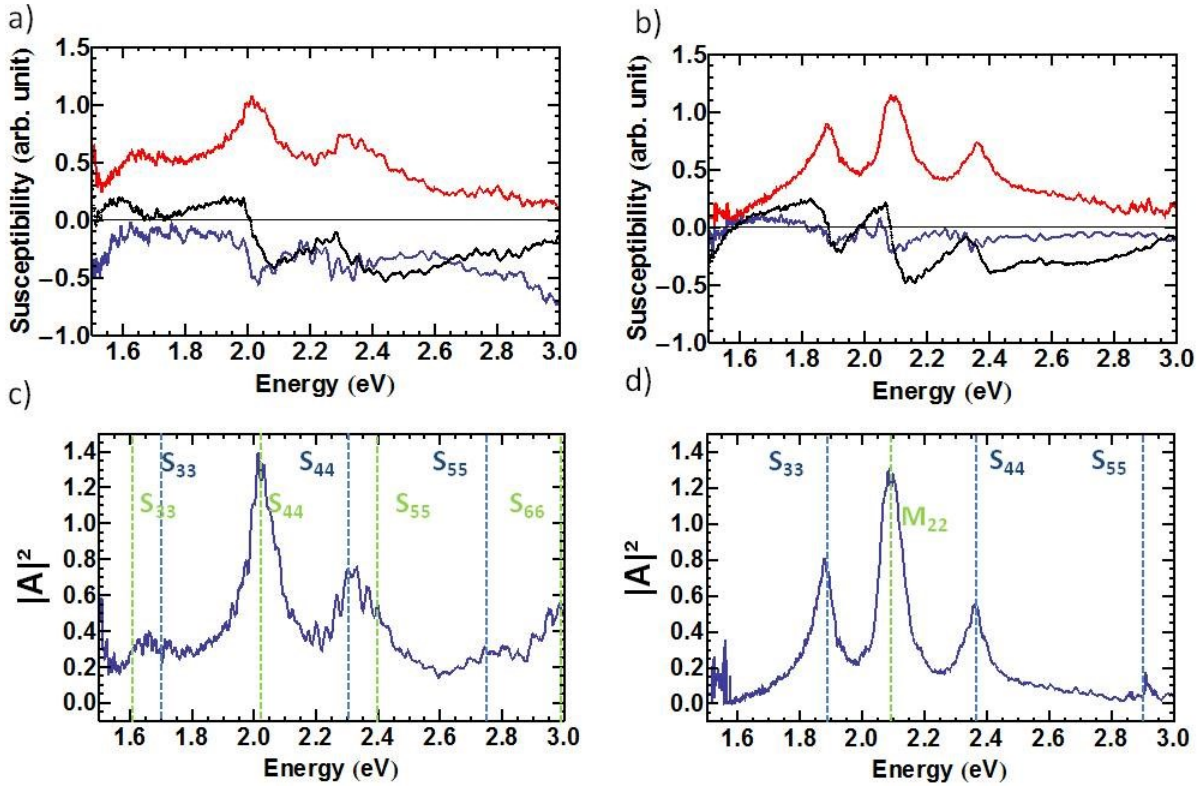

Figure 3. [a and b] Susceptibility extracted for (a) case A and (b) case B: Re(A) (blue line) and Im(A) (red line) extracted from our complete model. The black line represent Re(A) obtained from Kramers-Kronig transformation. [c and d] Reconstructed Rayleigh spectra free from depolarization and substrate effects using the developed model for (c) case A and (d) case B.

b. Imaging individual SWCNTs under real growth conditions

Our second study was devoted at demonstrating that individual SWCNTs could be imaged under real growth conditions (i.e., at atmospheric pressure, on a crystalline substrate) during their growth by HPOM. To do so, we first improved the optical setup by integrating a spatial filter (to reduce the beam dispersity), engineered the injection of the beam in the objective (to enlarge the field of view) and added a long-distance objective with high polarization conservation (to focus on the sample surface inside a miniaturized CVD cell) (Figure 4a). The growth conditions (temperature, pressure of ethanol used as carbon precursor) were then optimized to allow the growth of long individual SWCNTs parallel to the [100] axis of the ST-cut quartz substrate. Lines of catalyst (iron nanoparticles) and optical markers were also patterned on the substrates by UV lithography. The configuration of the CVD cell and the

substrate were finally optimized to reduce the back reflection of light through the birefringent substrate which strongly reduces the image contrast in this polarization-based method.

Figure 4b shows snapshots of a typical *in situ* video obtained during the growth of individual SWCNTs after optimization. One can clearly observe individual SWCNTs growing from the catalyst pattern at different rates and for different lifetimes. Such images under real growth conditions are a world first. Before that, it was possible to image individual SWCNTs (even with atomic resolution) by *in situ* TEM but only under unrealistic growth conditions (low pressure, no substrate) and limited to the zone of the catalyst-nanotube interface.

Our observations showed that, contrary to previous beliefs based on measurements on nanotube ensembles, the growth rate of individual SWCNTs does not display an exponential decay over time. At the opposite, individual SWCNTs grow at a constant growth rate until a sudden termination event (Figure 4c). Because SWCNTs display a large dispersion of lifetimes, an exponential decay appears when summing the behaviors of individual SWCNTs, in good analogy for instance with radioactive decay. This exponential decay is therefore the signature of an ensemble of nanotubes, by opposition to that of individual SWCNTs.

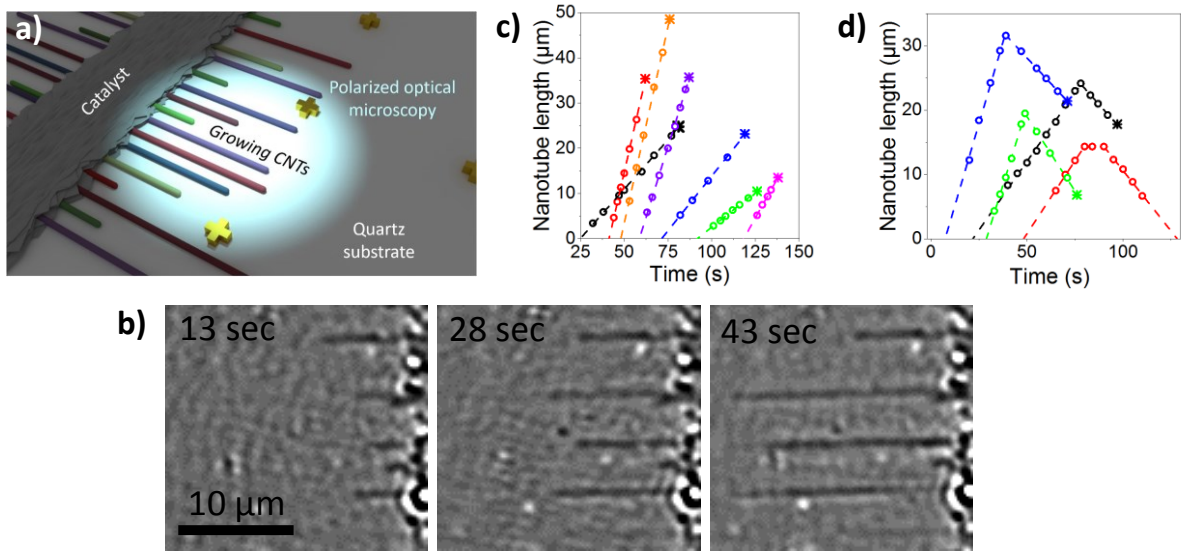

Figure 4. a) Illustration of the in situ imaging of individual SWCNTs by HPOM during their [100]-oriented growth on a quartz substrate. b) Video snapshots of individual SWCNTs growing from a patterned catalyst line (on the right side). c) Length of individual SWCNTs versus time during standard growth. d) Length of individual SWCNTs versus time in the special case of individual SWCNTs switching from growth to etching. In figures c and d, the "X" symbol denotes termination.

Based on these observations, we performed a statistical analysis of the growth rates and lifetimes of individual SWCNTs, which showed a large dispersion: in constant growth conditions, growth rates can vary by a factor 20 and lifetimes by a factor 50 (Figure 4a). Interestingly, the lifetime appears inversely related to the growth rate, which supports that the limiting step of nanotube growth is also responsible for the abrupt growth termination. This inverse relationship is also observed when changing the temperature or the precursor pressure: when increasing the temperature or the precursor pressure, the growth rates tend to increase while the lifetimes tend to decrease (Figures 5b,c). This is an important result for chiral selectivity because it supports that a chiral selectivity simply based on growth kinetics may simply not be possible (at least in the conditions of our study) since the length gain from a higher growth rate is statistically countered by a reduced lifetime.

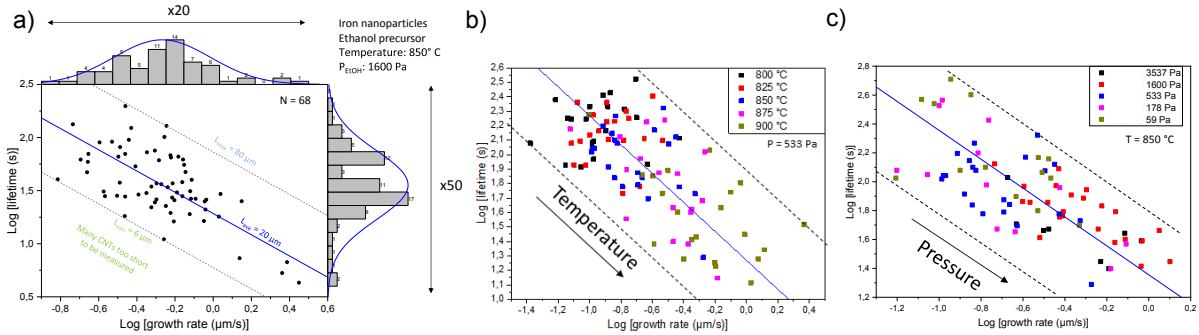

Figure 5. Distribution of lifetimes versus growth rates on a logarithmic scale for (a) constant growth conditions, b) with increasing growth temperature, c) with increasing pressure of carbon precursor.

Beside the main behavior of nanotubes growing at a constant rate until sudden termination, some tubes were surprisingly observed to switch from growth (increasing length) to etching (decreasing length) (Figure 4d). Like the growth rate, the etching rate was also observed to remain constant with time. Like growth, this etching occurs at the interface between the nanotube and the catalyst particle, and is therefore named catalytic etching (by opposition to standard etching which occurs all along the nanotube length). We think that this catalytic etching is caused by mild etchants present in the gas phase. We actually observed an increase of the water concentration during growth which we could track down to two effects: i) water traces dissolved in liquid ethanol, and ii) water molecules resulting from the decomposition of ethanol at high temperature. The switch can be explained by a threshold concentration ratio between carbon precursors and etchant molecules. Interestingly for nanotube selectivity, this threshold appears to vary from tube to tube, and, while some tubes shift to etching (and then disappear), other tubes keep growing at unchanged rate. However, the exact relationship with the nanotube chirality remains to be elucidated.

c. Chiral selectivity of nanotube growth controlled by catalytic etching

Our third study was devoted at relating the growth kinetics measured for individual SWCNTs with the chiral structure of the SWCNTs (diameter and chiral angle). To do so, we performed a statistical analysis of the chiral structure of the SWCNTs by Raman spectroscopy at different wavelengths. Identifying nanotube structure can be done using Raman features such as the radial breathing mode (RBM, at low frequency at around 100-350 cm^{-1}) and the G band (at high frequency at around 1300-1600 cm-1). Using Raman spectroscopy, the defect density can also be assessed based on the relative intensity of the D band (at around 1300-1350 cm-1). This statistical study also allowed us to adapt the Kataura plot used for chirality assignments (*i.e.* the diagram relating the nanotube structure with its RBM frequency and optical transitions) to the environment of the nanotubes (quartz substrate), and therefore to improve the accuracy of chirality assignment.

Standard theory (*25*) currently states that nanotubes with chiral angles of 19° should be the most reactive (*i.e.* having the highest density of reactive sites at the nanotube edge) and therefore display the highest growth rates. At the opposite, nanotubes with chiral angles of 0° (zigzag) and 30° (armchair) should display the slowest growth rates. Note that this notion of reactivity applies both to carbon integration (growth) and carbon removal (etching) as already shown in the case of graphene. As shown in figure 6a, our experimental results actually reveal a behavior exactly opposite to that predicted by standard (but too simple) theory. This can be rationalized by considering that, under real conditions, carbon integration at the nanotube edge is in competition with carbon etching: if carbon incorporation is not selective in chiral angle

(*i.e.* isotropic) as likely considering the high carbon supply used in our experiments (around 16 000 ppm) while carbon etching is selective due to the low concentration of water experimentally measured (around 300 ppm), it follows that the most reactive nanotubes (e.g. with chiral angles of 19°) will display the highest etching rate and therefore the slowest effective growth rates. This hypothesis is additionally supported by the variation of the defect density with chiral angle. Actually, it is expected that a high rate of carbon etching at the nanotube edge would leave traces in the nanotube structure, such as a higher density of defects (*e.g.* vacancies or oxygen-containing defects) in the nanotube wall. This is exactly what is observed: as shown in Figure 6b, the G/D ratio (which is inversely related to the defect density) follows the same trend with chiral angle as the growth rate, meaning that the slowest-growing tubes with intermediate chiral angles are also the most defective ones.

These results are of paramount importance because they show that the chiral selectivity of nanotube growth can be controlled by catalytic etching instead of carbon incorporation. Here, it is important to note that etchants such as water or oxygen are present in most nanotube growth conditions either as controlled ingredients (e.g. oxygen-containing carbon precursors such as ethanol, controlled addition of water) or as unwanted contaminants. We therefore suspect that catalytic etching plays a major role in most of the chiral selective methods reported to date. If carefully controlled, catalytic etching offers a novel and powerful degree of freedom for engineering chiral selection. As shown in figure 4d, catalytic etching may not only be used to slow the growth of some specific tubes but even to completely remove them by switching them from growth to etching.

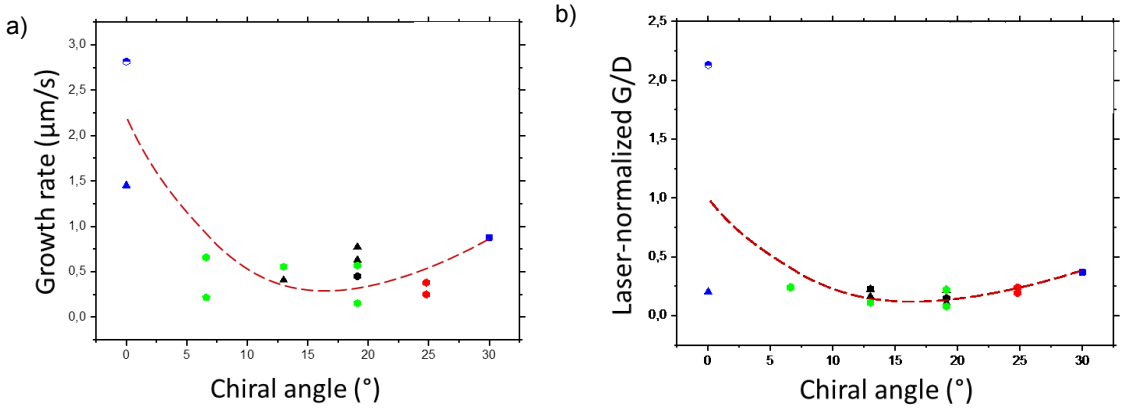

Figure 6. a) Growth rate versus chiral angle. b) Laser-normalized G/D ratio versus nanotube chiral angle.

3. Publications and conference presentations from the project

Publications:

- "Comprehensive model of the optical spectra of carbon nanotubes on a substrate by polarized microscopy", Léonard Monniello, Huy-Nam Tran, Rémy Vialla, Guillaume Prévot, Said Tahir, Thierry Michel, and Vincent Jourdain, Physical Review B 99, 115431 (2019)
- "Direct imaging of individual single-walled carbon nanotubes under real growth conditions using *in situ* polarized optical microscopy", Huy-Nam Tran, Léonard Monniello, Vladimir Pimonov, Said Tahir, Thierry Michel, and Vincent Jourdain, in preparation.

- "Chiral selectivity of SWCNT growth controlled by catalytic etching", Vladimir Pimonov, Huy-Nam Tran, Said Tahir, Thierry Michel, and Vincent Jourdain, in preparation.

Conference presentations:

- "Studying the growth of single-walled carbon nanotubes by optical means", V. Jourdain et al., **NT19**, Wurzburg, Germany, July 2019.
- "Studying the growth of single-walled carbon nanotubes by optical means", V. Jourdain et al., **MRS Fall Meeting**, Boston, USA, November 29, 2018.
- "Studying the growth of single-walled carbon nanotubes by optical means", V. Jourdain et al., **GDR-I Graphene and Co**, Aussois, France, October 2017.

4. References

1. M. Su *et al.*, Lattice-Oriented Growth of Single-Walled Carbon Nanotubes. *J. Phys. Chem. B*. **104**, 6505–6508 (2000).
2. Y. Hu *et al.*, Growth of high-density horizontally aligned SWNT arrays using Trojan catalysts. *Nat. Commun.* **6**, 6099 (2015).
3. M. M. Shulaker *et al.*, Three-dimensional integration of nanotechnologies for computing and data storage on a single chip. *Nature*. **547**, 74–78 (2017).
4. Q. Cao *et al.*, End-bonded contacts for carbon nanotube transistors with low, size-independent resistance. *Science*. **350**, 68–72 (2015).
5. C. Qiu *et al.*, Scaling carbon nanotube complementary transistors to 5-nm gate lengths. *Science*. **355**, 271–276 (2017).
6. S.-J. Han *et al.*, High-speed logic integrated circuits with solution-processed self-assembled carbon nanotubes. *Nat Nano*. **12**, 861–865 (2017).
7. T. Simonite, IBM: Commercial Nanotube Transistors Are Coming Soon. *MIT Technol. Rev.* (2014).
8. R. C. Johnson, China Takes Lead in Carbon Nanotubes & Graphene. *EETimes* (2014).
9. A. D. Franklin, Electronics: The road to carbon nanotube transistors. *Nature*. **498**, 443–444 (2013).
10. M. M. Shulaker *et al.*, Carbon nanotube computer. *Nature*. **501**, 526–530 (2013).
11. Q. Cao *et al.*, Arrays of single-walled carbon nanotubes with full surface coverage for high-performance electronics. *Nat. Nanotechnol.* **8**, 180–186 (2013).
12. L. Kang *et al.*, Growth of close-packed semiconducting single-walled carbon nanotube arrays using oxygen-deficient TiO2 nanoparticles as catalysts. *Nano Lett.* **15**, 403–409 (2015).
13. L. Kang, S. Zhang, Q. Li, J. Zhang, Growth of horizontal semiconducting SWNT arrays with density higher than 100 tubes/μm using ethanol/methane chemical vapor deposition. *J. Am. Chem. Soc.* **138**, 6727–6730 (2016).
14. W. Zhou, S. Zhan, L. Ding, J. Liu, General rules for selective growth of enriched semiconducting single walled carbon nanotubes with water vapor as in situ etchant. *J. Am. Chem. Soc.* **134**, 14019–14026 (2012).
15. F. Yang *et al.*, Chirality-specific growth of single-walled carbon nanotubes on solid alloy catalysts. *Nature*. **510**, 522–524 (2014).
16. V. I. Artyukhov, E. S. Penev, B. I. Yakobson, Why nanotubes grow chiral. *Nat. Commun.* **5**, 4892 (2014).

17. F. Ding, A. R. Harutyunyan, B. I. Yakobson, Dislocation theory of chirality-controlled nanotube growth. *Proc. Natl. Acad. Sci. U. S. A.* **106**, 2506 (2009).
18. L. Monniello *et al.*, Comprehensive model of the optical spectra of carbon nanotubes on a substrate by polarized microscopy. *Phys. Rev. B*. **99**, 115431 (2019).
19. D. Y. Joh *et al.*, On-Chip Rayleigh Imaging and Spectroscopy of Carbon Nanotubes. *Nano Lett.* **11**, 1–7 (2010).
20. R. W. Havener, A. W. Tsen, H. C. Choi, J. Park, Laser-based imaging of individual carbon nanostructures. *NPG Asia Mater.* **3**, 91 (2011).
21. W. Wu *et al.*, True-color real-time imaging and spectroscopy of carbon nanotubes on substrates using enhanced Rayleigh scattering. *Nano Res.* **8**, 2721–2732 (2015).
22. J. Lefebvre, P. Finnie, Polarized light microscopy and spectroscopy of individual single-walled carbon nanotubes. *Nano Res.* **4**, 788 (2011).
23. K. Liu *et al.*, High-throughput optical imaging and spectroscopy of individual carbon nanotubes in devices. *Nat Nano*. **8**, 917–922 (2013).
24. S. Deng *et al.*, High-Throughput Determination of Statistical Structure Information for Horizontal Carbon Nanotube Arrays by Optical Imaging. *Adv. Mater.* **28**, 2018–2023 (2016).
25. E. S. Penev, K. V Bets, N. Gupta, B. I. Yakobson, Transient kinetic selectivity in nanotubes growth on solid co–w catalyst. *Nano Lett.* **18**, 5288–5293 (2018).